



# Computational Expedition into Antibacterial Drug Discovery: In-Silico Design and Docking Studies of Novel Ciprofloxacin-1,3,4-Thiadiazole Derivatives

Yogesh Matta<sup>1\*</sup>, Jagdish Kumar Arun<sup>2</sup>, Saurabh Gupta<sup>3</sup>, Shikhar Rathore,<sup>4</sup>Harsha Parihar<sup>4</sup>, Varsha Gupta<sup>5</sup>

<sup>1</sup>School of Pharmacy Suresh Gyan Vihar University Jayapura, Jaipur (Rajasthan)-India

<sup>2</sup>Faculty of Pharmaceutical Science and Nursing, Department of Pharmacy Vivekananda Global University Jagatpura, Jaipur (Rajasthan)-India

<sup>3</sup>Chameli Devi Institute of Pharmacy, Khandwa Road, Indore (M.P.)-India

<sup>4</sup>Mathura Devi Institute of Pharmacy, Indore (M.P.)-India

<sup>5</sup>NMT Gujrati College of Pharmacy, Indore (M.P.)-India

(Received: 04 February 2024

Revised: 11 March 2024

Accepted: 08 April 2024)

## KEYWORDS

Antibacterial,  
*Salmonella typhi*  
OmpF,  
*Escherichia coli*  
MenB  
Drug Design,  
Molecular Docking,  
Ciprofloxacin,  
1,3,4-Thiadiazole,  
Computational  
Analysis

## ABSTRACT:

**Introduction** The research work focused on the in-silico design and docking studies of novel derivatives of Ciprofloxacin fused with 1,3,4-thiadiazole moieties as potential antibacterial agents. The rationale behind this computational expedition was to harness the benefits of rational drug design and molecular docking to enhance the antibacterial activity of Ciprofloxacin, a widely used fluoroquinolone antibiotic.

**Objectives:** Employing advanced in-silico methods, a range of derivatives was developed and analysed through molecular docking simulations against specific bacterial targets. The binding affinities and interaction patterns of these derivatives with essential bacterial enzymes or proteins were completely investigated using computational methods

**Methods:** The study revealed promising outcomes, highlighting several derivatives that exhibited heightened binding affinities, suggesting a potential for enhanced antibacterial efficacy compared to the original compound, ciprofloxacin. Particularly noteworthy were structural alterations in the 1,3,4-thiadiazole component, showing significant impacts on the binding interactions, offering promising avenues for personalized drug design strategies against bacterial infections.

**Results:** The identified compounds from this study hold promise for future development as potent antibacterial drugs, contributing to the ongoing efforts to combat antibiotic resistance and address the pressing need for novel therapeutic options in the field of infectious diseases.

**Conclusions:** The study aimed to enhance the antibacterial activity of Ciprofloxacin by designing and docking novel derivatives with 1,3,4-thiadiazole moieties. Advanced in-silico methods were used to analyze binding affinities and interaction patterns with bacterial targets. The results showed promising outcomes, with several derivatives showing heightened binding affinities. Structural alterations in the 1,3,4-thiadiazole component showed significant impacts on binding interactions.



## Introduction:

Bacterial infections pose severe risks to human health, capable of impacting any organ within the body. Each bacterial species tends to exhibit a preference for specific organs, selectively infecting them [1]. Thriving in diverse environments, bacteria play crucial roles in maintaining environmental balance. Notably, diseases and infections arise from a fraction of the vast array of bacterial species on Earth. The ramifications of these illnesses on public health are substantial. Unlike viral illnesses, bacterial infections are generally more manageable due to the wider availability of antibacterial resources. However, the emergence of antimicrobial resistance presents a pressing concern for researchers [2]. Bacteria stand out among prokaryotic species, as many can coexist within the body without causing infections; instead, they contribute to regulating the body's flora. Visible infections represent only a small subset of the overall instances of bacterial presence [3]. Transmission of bacterial diseases occurs through various means, often requiring specific organisms to reach susceptible hosts for infection. Bacteria have adapted across water, soil, food, and various environments, employing diverse strategies, including the utilization of vectors, to infect humans [4].

Contrary to common perception, most bacteria are non-threatening to humans, with certain types proving beneficial. Within the human gastrointestinal tract, beneficial bacteria aid digestion, synthesize essential vitamins, and bolster immunity by fortifying the body against harmful bacteria and infections. It's important to note that among the vast array of bacterial strains, only a small fraction have the potential to cause illness in humans [5]. The pathogenesis of bacterial infections involves the initiation of the infectious process and the mechanisms driving the emergence of signs and symptoms of illness. Pathogenic bacteria possess specific traits contributing to their virulence, including transmissibility, the capacity to adhere to host cells, persistence within the host, invasion of host tissues, toxigenicity, and evasion or survival tactics against the host's immune system [6]. Additionally, resistance to antimicrobials and disinfectants can further enhance an organism's virulence, amplifying its ability to induce disease. Interestingly, many infections caused by bacteria commonly recognized as pathogens may go

unnoticed or present as asymptomatic, adding complexity to their detection and management [7].

An antibacterial agent serves to either impede the growth of bacteria or eradicate them completely. Antibiotics, a cornerstone in contemporary medicine, work by either killing or suppressing bacterial activity, offering a widely employed treatment approach [8]. The accidental discovery of penicillin by Alexander Fleming from *Penicillium notatum* stands as a pivotal event in medical history, marking the inception of antibiotics. Initially hailed as a breakthrough, penicillin represented a diverse array of antibiotics capable of both treating and preventing bacterial illnesses. Over time, however, their overuse led to the development of resistance, leading to their diminished effectiveness and eventual phasing out [9].

Antibiotics have historically been lauded as "wonder drugs" for their ability to effectively combat and prevent bacterial infections. For decades, they served as potent and widely utilized medications, proving instrumental in treating various bacterial infections across the globe. Since their serendipitous discovery around fifty years ago, antibiotics have been credited with saving millions of lives, representing a cornerstone in the fight against infectious diseases [10-12].

Drug development is an ever-evolving field that hinges on continual innovation and technological progress, blending both computational and experimental methodologies [13]. Leveraging bioinformatics tools, in-silico techniques play a pivotal role in identifying potential drug targets. This involves utilizing knowledge regarding the structural and physicochemical aspects of receptor-ligand interactions [14-16]. In computer-aided drug design (CADD), these insights are harnessed to identify target structures, pinpoint potential active sites, generate candidate molecules, assess their similarity, dock them with the target, rank them based on their binding affinities, and subsequently refine and optimize these molecules to enhance their binding characteristics. Structure-based drug design, also known as the direct approach (SBDD), is predominantly utilized when the three-dimensional structure of disease-related targets is known [17-21]. This method involves molecular docking and de novo ligand design. Molecular docking predicts how drug molecules bind to protein targets and determines their binding strength or "score." This process



is crucial in the rational design of drugs, aiming to find the optimal conformation for both the protein and the ligand to minimize the system's free energy. Following this, synthesized compounds undergo biological testing [21-26].

### Methodology:

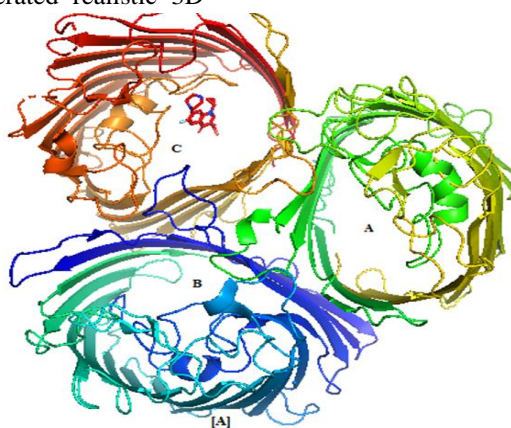
**Data Collection:** Carefully selected studies that employed similar docking methodologies and shared common evaluation metrics to compile the dataset. Relevant data, such as protein structures, ligand information, and experimentally determined binding affinities, were extracted from these papers. To ensure reliability and consistency, we thoroughly cross-referenced the data and excluded studies with incomplete or ambiguous information. By organizing data from various sources, we created a comprehensive dataset that serves as a valuable tool for evaluating and comparing our own docking algorithms.

**Structure Preparation:** In this research, the preparation of both 2D and 3D structures was performed using ChemDraw software. ChemDraw is a powerful molecular drawing tool widely used in the field of computational chemistry and drug discovery. For the 2D structure preparation, the chemical compounds of interest were visually depicted using ChemDraw's intuitive interface. The software provided a comprehensive set of drawing tools, allowing us to accurately represent the atoms, bonds, and functional groups present in the molecules. Once the 2D structures were created, ChemDraw facilitated the conversion of these representations into their corresponding 3D structures. Through the utilization of various algorithms and force fields, the software generated realistic 3D

conformations that accounted for the spatial arrangement of atoms in the molecules.

The minimization of energy for 3D structures was executed using ChemDraw 3D software equipped with MM2 (Merck Molecular Force Field). Energy minimization holds great significance in the realm of computational chemistry as it aims to enhance the conformation of a molecule by reducing its potential energy. ChemDraw 3D offers a comprehensive set of tools and algorithms that effectively facilitate this process. Initially, the 3D structures, generated either through experimental data or computational methods, were imported into ChemDraw 3D for further enhancement. The software utilized force fields such as MMFF (Merck Molecular Force Field) or AMBER (Assisted Model Building with Energy Refinement) to compute the energy of the molecule and determine the optimal positions for the atoms. These force fields take various factors into account, including bond lengths, bond angles, and torsional angles, in order to evaluate the potential energy of the system.

**Protein Preparation:** The literature search guided the selection of two key proteins for docking research. The first, PDB ID 4KRA, represents the crystal structure of Salmonella typhi OmpF, coupled with Ciprofloxacin (CPF) as a co-crystallized ligand. This membrane protein, resolved at 3.32, holds significance in antibacterial activity (Figure 1). The second, PDB ID 3T88, showcases the crystal structure of Escherichia coli MenB along with a substrate analog (SON) as a co-crystallized ligand—an identified target notable for its relevance in antibacterial activity, resolved at 2.00 (Figure 2).



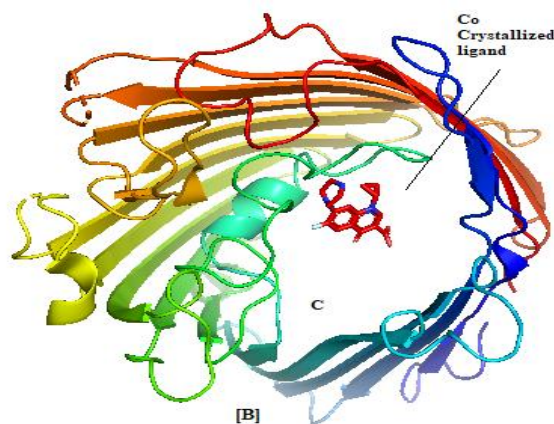


**Figure 1:** [A] Protein Structure with co-crystallized ligand PDB ID: 4KRA  
[B] Chain C with co-crystallized ligand S0N

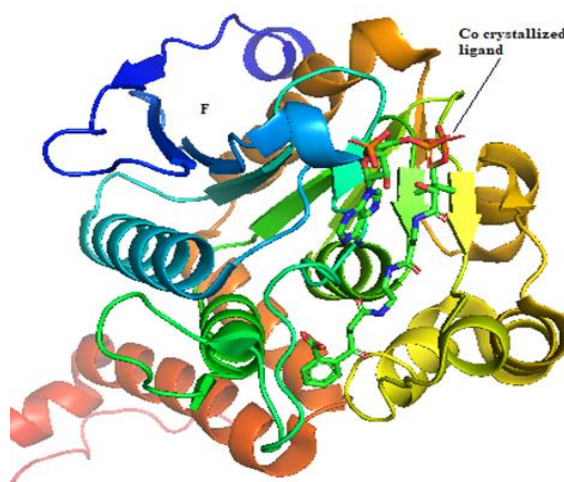


**Figure 2:** Crystal structure of Protein with co-crystallized ligand PDB ID: 3T88

In this study, the crystal structures of proteins (**PDB IDs: 4KRA & 3T88**) were retrieved from the Protein Data Bank (PDB) using their assigned scientific codes. **Molegro Virtual Docker (MVD)** was employed for protein preparation, utilizing its preparation wizard to rectify any potential issues such as missing hydrogens and charges. The initial PDB files contained three-dimensional coordinates of the protein structures, from which non-protein elements like water molecules and ligands were removed to focus solely on the protein. Any missing atoms were added, and structural irregularities were addressed before energy optimization and structural enhancement using Autodock. Kollman charges, specific charges based on the Kollman force field, were assigned to each protein atom. This allowed the software to

simulate protein interactions during docking simulations, providing deeper insights into these interactions.

**Ligand preparation** - The ligands (Designed 1,3,4-thiadiazole derivatives of Ciprofloxacin) listed in Table, were drawn using the ChemDraw Ultra 12. Chem3D was used to minimize the energy of the ligands and the resulting structure had minimum energy. The optimized ligands were saved in PDB file format and then imported into the Molegro Virtual Docker (MVD), where they were prepared with the help of the MVD's preparation wizard (capable of repairing possible missing hydrogens and charges).

**Designing:** Designing compounds involved an extensive literature search focusing on ciprofloxacin and



1,3,4-thiadiazole derivatives. Twenty-five compounds were designed by incorporating diverse substitutions at various positions within the piperazine ring of ciprofloxacin and the benzene ring linked to the

thiadiazole nucleus. The structural representations were created using ChemDraw software and are detailed in Table 1.

### Synthetic scheme for the ciprofloxacin 1,3,4-thiadiazole conjugates and their design strategy

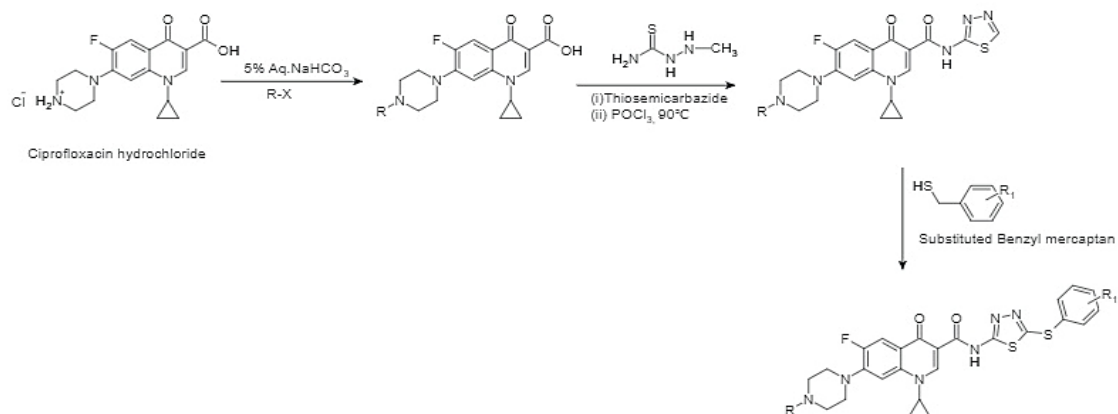
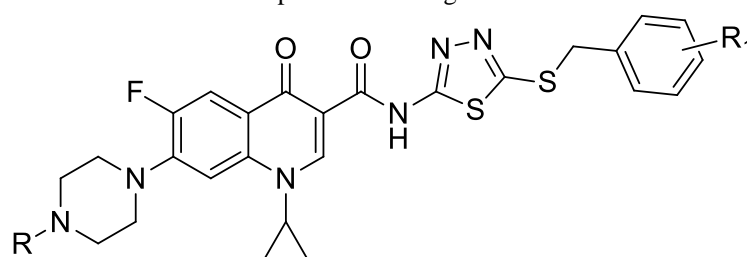


**Table 1:** Represent the designed molecules:



S. No.	Molecules	Structure	R	R <sub>1</sub>
1.	D1		-CH <sub>3</sub>	3-CF <sub>3</sub>
2.	D2		-Cl	2-Cl



3.	D3		-F	-H
4.	D4		-CH <sub>3</sub>	2-F
5.	D5		-Br	-H
6.	D6		-CH <sub>3</sub>	2-CH <sub>3</sub>
7.	D7		-OCH <sub>3</sub>	4-OCH <sub>3</sub>
8.	D8		-H	2,4-NO <sub>2</sub>



9.	D9		-H	2-NO <sub>2</sub>
10.	D10		-H	3-NO <sub>2</sub>
11.	D11		-CH <sub>3</sub>	4-NO <sub>2</sub>
12.	D12		-H	2-SH
13.	D13		-C <sub>2</sub> H <sub>5</sub>	4-hexyloxy
14.	D14		-CH <sub>3</sub>	4-tertbutyl
15.	D15		-NO <sub>2</sub>	-H



16.	D16		-NO <sub>2</sub>	2-NO <sub>2</sub>
17.	D17		-CH <sub>3</sub>	2,4-Br
18.	D18		-H	4-CF <sub>3</sub>
19.	D19		-H	4-OCH <sub>3</sub>
20.	D20		-H	Pyridine in place of Benzene
21.	D21		-OCH <sub>3</sub>	3-CF <sub>3</sub>
22.	D22		-C <sub>3</sub> H <sub>7</sub>	4- hexyloxy



23.	D23		-C <sub>2</sub> H <sub>5</sub>	2,4,6-NO <sub>2</sub>
24.	D24		- Tertbutyl	4-aminoethyl
25.	D25		-CH <sub>3</sub>	2,4-Cl

**Docking Methodology:** The docking methodology involved several steps. Initially, proteins were downloaded in .pdb format from the RCSB PDB and imported into the workspace. The protein and ligand were visualized, and a surface was generated to understand the protein's structure. The system automatically detected the protein's binding site, visualized in the simulation structures tab. For setting up the docking simulation, various options were available in the Setup Docking wizard tab. Default settings were initially utilized. The docking progress was monitored through the Molegro Virtual Docker Batchjob box, and the obtained poses were stored in the specified output directory upon completion.

To import the docking results into MVD, the Docking Results (.mvdresults) file was used through the File menu or by dragging it into the MVD software. Following the import, the Ligand map was accessed to visualize the 2D interactions between the protein and ligand. Finally, the docking results were visualized using Pymol visualizing software, showcasing the outcome of the target protein in table.

**1) Docking Parameters:** The parameters employed for the docking simulation involved utilizing the

MolDock score, known for its speed and accuracy, as the scoring function. A grid resolution of 0.3 Å was set, and the docking radius was expanded to 15 to encompass the gaps within the protein structure. The docking algorithm, MolDock SE (Simplex Evolution), was utilized with specific settings enabled: constrained poses to the cavity, energy minimization, and optimization of H-bonds boxes. Additionally, within the simplex evolution, parameters such as a Max step of 300 and a neighbor distance factor of 1.00 were applied. Pose clustering was implemented to ensure a diverse range of binding modes.

**2) MolDock score:** The MolDock scoring function enhances the piecewise linear potential (PLP) by introducing additional factors related to hydrogen bonding and electrostatic attraction. To focus on relevant atoms, the "ignore-distant-atom" command disregards those far from the binding site. Directionality for hydrogen bonding is assessed to determine potential donors and acceptors. The protein's binding site was delineated by expanding the radius to 15 Å, encompassing the cavity along the X, Y, and Z axes. The dimensions of the binding cavities were determined using the MVD docking



wizard: for 4KRA, X= -27.74, Y= 20.88, Z= -46.75, and for 3T88, X= -38.58, Y= 30.62, Z= -2.43.

**3) Re-rank score:** Re-ranking scoring functions play a pivotal role in crafting and predicting molecular models used for computing chemical properties. Compared to the docking simulation scoring function, the score function in re-ranking is more intricate computationally. However, it typically outperforms the docking score function when it comes to determining the best pose among numerous poses of a particular ligand. While the MVD re-rank score gauges the strength of the interaction between the ligand and protein, it lacks calibration in chemical units and doesn't encompass complex contributions like entropy.

**4) Docking simulation:** The simulation of the docking model serves the purpose of identifying interactions between designed compounds and a specific active target site. In this case, 25 derivatives of Ciprofloxacin 1,3,4-thiadiazole derivatives were subjected to docking simulations with the binding sites of Salmonella typhi OmpF and Escherichia coli MenB proteins (PDB ID: 4KRA & 3T88) obtained from the Protein Data Bank. To evaluate the docking, a computational approach was employed using cc to determine the interaction energy between the compounds and their respective target proteins. This involved importing a saved file into the Molegro Virtual Docker, which utilizes its cavity detection algorithm to delineate the binding pocket within the model.

**5) Drug likeness and in-silico ADMET prediction:** Advancements in computational technology have

significantly reduced the necessity for extensive experimental drug trials while boosting their success rates, establishing it as a pivotal tool in identifying potential drug candidates. To assess the behavior of ligands within the human body, their pharmacokinetic properties—absorption, distribution, metabolism, excretion, and toxicity (ADMET)—are scrutinized.

For this analysis, the ADMET characteristics of the ligands were investigated using SwissADME, an online tool specialized in predicting ADME properties (accessible at <http://www.swissadme.ch>). Predicting the drug-likeness of these compounds involved employing Lipinski's Rule of Five, a foundational criterion for evaluating the potential of new molecular entities (NMEs) as viable drugs.

This rule establishes key parameters for drug-likeness. According to Lipinski's Rule, molecules surpassing thresholds of more than 5 H-bond donors, 10 H-bond acceptors, a molecular weight beyond 500 Da, or a computed Log P (CLog P) higher than 5 are deemed to have poor absorption or penetration as molecular entities.

**6) Validation of Docking Methodology:** The designed molecules exhibiting the best MolDock scores and re-rank scores were subsequently compared with standard drugs such as ciprofloxacin and ampicillin. Remarkably, these designed compounds demonstrated superior binding affinities compared to the standard drugs. Table 5 illustrates the docking scores of the standard drugs alongside their amino acid interactions for reference.

**Table 5:** Validation of designed molecules with standard drugs:

Standard Drug	Software	PDB ID	Mol Dock score	Re rank score	H-Bond	Amino acid Interactions
Ciprofloxacin	Molegro Virtual Docker 6.0	4KRA	-103.611	-89.1354	-4.81304	Tyr101, Tyr97, Ser114
Ciprofloxacin	Molegro Virtual Docker 6.0	3T88	-93.9283	-74.7226	-2.00199	Leu229, Lys233



Ampicillin	Molegro Virtual Docker 6.0	3T88	-106.037	-63.286	-4.16611	Arg64, Thr117, Gln248, Asn252
------------	----------------------------	------	----------	---------	----------	-------------------------------

To confirm the reliability of the docking results, we specifically selected two drugs, Ciprofloxacin and Ampicillin, and conducted docking experiments using the same targets, 4KRA and 3T88. We then compared the docking scores obtained from these standard drugs with the scores from the best molecules, specifically D14 and D23 for 4KRA, and D17 and D23 for 3T88. Upon comparison, the docking results were found to be consistent and comparable with the scores obtained from the standard drugs.

Remarkably, compounds D14 and D23 (for 4KRA) and D17 and D23 (for 3T88) displayed notably better docking scores in comparison to the standard drugs, Ciprofloxacin and Ampicillin.

**Result and Discussion:** In the docking process, the crystal structures of Salmonella typhi OmpF and Escherichia coli proteins were engaged with the ligands. Each ligand sought out the most favorable location within the structure, where subsequently the re-rank score was computed. The best poses in each docking iteration were chosen based on their re-rank scores. Tables 2 and 3 present the MolDock scores and re-rank scores of the optimal poses obtained in the docking studies involving the ligands, specifically the Ciprofloxacin 1,3,4-thiadiazole derivatives, interacting with the target proteins PDB ID 4KRA and 3T88, respectively.

**Table 2:** Docking result of the target protein using Molegro Virtual Docker. (PDB ID-4KRA):

S. No.	Molecules	Mol Dock Score	Re-rank Score	H-Bond
1.	D1	-126.255	-96.4908	-0.274371
2.	D2	-126.347	-94.2476	-2.5
3.	D3	-113.902	-85.694	-1.62494
4.	D4	-108.936	-78.8857	-2.15635
5.	D5	-125.908	-94.8146	-2.15625
6.	D6	-117.769	-91.3419	-2.28916
7.	D7	-129.183	-82.1563	-4.33847
8.	D8	-141.854	-89.3751	-10.3472
9.	D9	-120.632	-96.2729	-2.76139
10.	D10	-129.529	-102.989re	-2.75396
11.	D11	-120.535	-92.249	-5.00442
12.	D12	-116.06	-91.1062	-7.13456
13.	D13	-134.286	-88.9432	-8.38806
14.	D14	-154.547	-109.901	-8.28603
15.	D15	-120.98	-94.9763	-6.49073



16.	D16	-115.458	-101.173	-0.838776
17.	D17	-137.726	-99.1913	-6.24955
18.	D18	-141.912	-102.046	-7.85801
19.	D19	-129.646	-93.4994	-8.10063
20.	D20	-113.625	-75.604	-3.1928
21.	D21	-130.71	-99.6124	-8.50859
22.	D22	-138.256	-81.8231	-2.7142
23.	D23	-142.085	-101.52	-7.30982
24.	D24	-134.622	-96.844	-8.01934
25.	D25	-134.552	-106.243	-2.73521

**Table 3:** Docking result of the target protein Using Molegro Virtual Docker PDB ID-3T88):

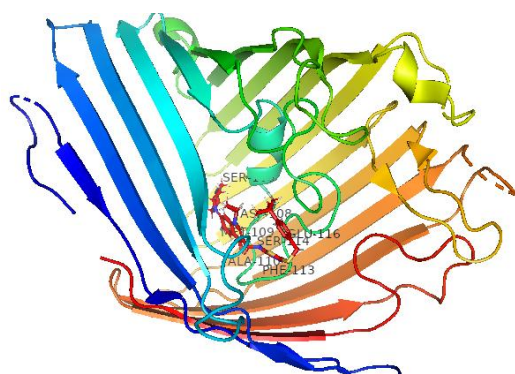
S. No.	Molecules	Mol Dock Score	Re-rank Score	H-Bond
1.	D1	-116.811	-74.7464	-3.04993
2.	D2	-104.222	-72.3995	-3.24735
3.	D3	-108.362	25.8481	0
4.	D4	-125.894	-80.1923	-2.92296
5.	D5	-107.088	-82.0545	-3.32145
6.	D6	-125.727	-57.8406	-5.61763
7.	D7	-107.386	66.4397	-0.941078
8.	D8	-124.928	-90.4685	-2.1858
9.	D9	-106.312	-62.3147	-2.61796
10.	D10	-114.17	-78.0642	-1.69077
11.	D11	-126.341	-73.4099	-3.67593
12.	D12	-107.883	-72.7737	-1.08524
13.	D13	-125.013	-73.3079	-2.27424
14.	D14	-129.694	-78.1959	-1.72729
15.	D15	-109.901	77.9002	-7.39873
16.	D16	-120.672	-78.2453	-4.14137
17.	D17	-130.676	-81.8404	-3.39418



18.	D18	-116.062	-74.5048	-2.18569
19.	D19	-110.856	-80.3479	-4.4921
20.	D20	-108.043	-68.3935	-4.89727
21.	D21	-114.785	-70.4906	-2.19868
22.	D22	-109.531	-35.8272	-2.86571
23.	D23	-126.828	-70.9183	-7.49519
24.	D24	-125.129	-82.3068	-0.869896
25.	D25	-122.838	-47.3879	-3.0262

According to molecular docking studies and interaction between protein and designed molecule D17 have Moldock score **-130.676** with amino acid interactions Arg64, Arg230, Glu248, Gln114, Thr117, and Asp110

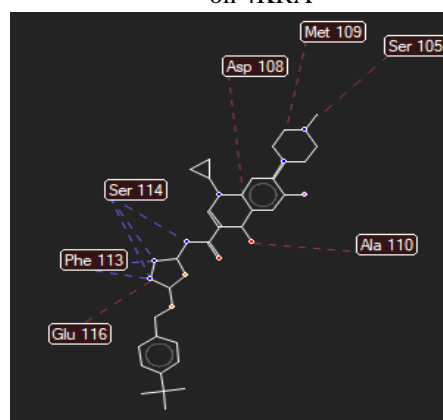
molecule D23 have Moldock score **-126.828** with amino acid interactions Thr117, Arg230, Asn252, Arg64, Asp110, Arg64, and Met25.



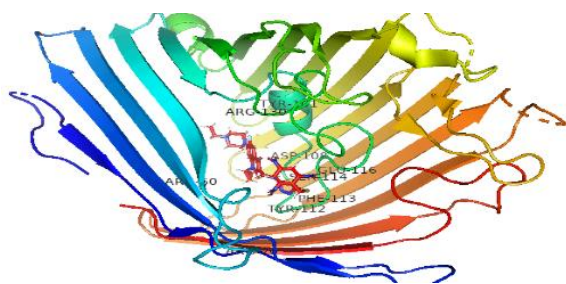
(a)

**Figure 6:** (a) Docked Image of Molecule D14 on 4KRA

**(b) Amino Acid Interaction of Molecule D14 on 4KRA**



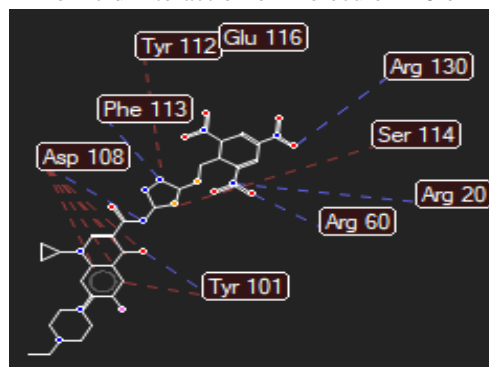
(b)



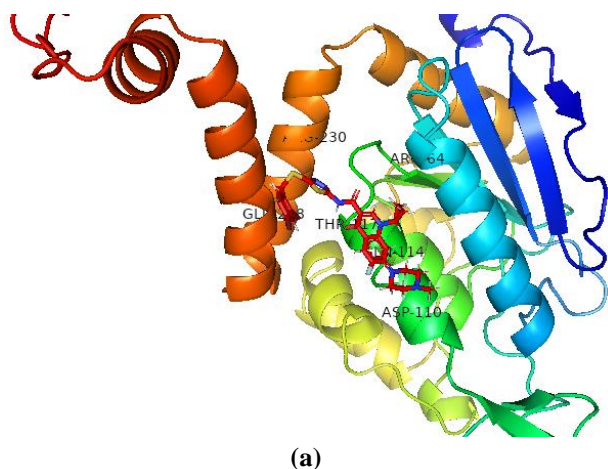
(a)

**Figure 7:** (a) Docked Image of Molecule D18 on 4KRA

**(b) Amino Acid Interaction of Molecule D18 on 4KRA**



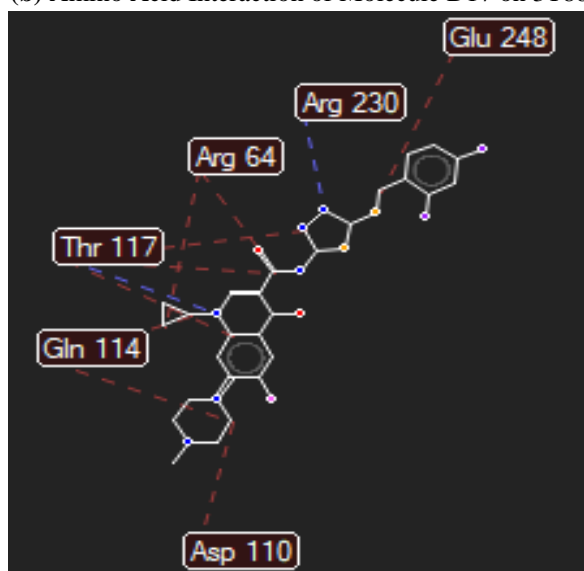
(b)



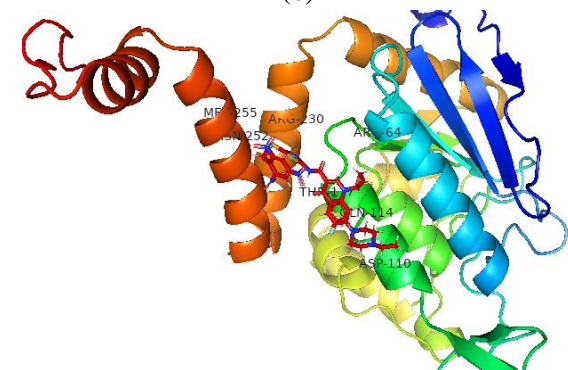
(a)

Figure 8: (a) Docked Image of molecule D17 on 3T88

(b) Amino Acid Interaction of Molecule D17 on 3T88



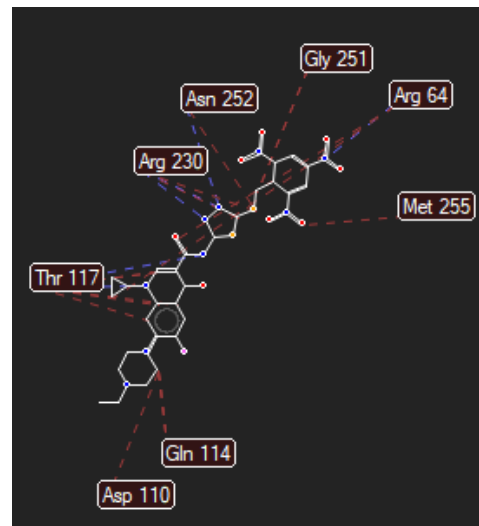
(b)



(a)

Figure 9: (a) Docked Image of molecule D23 on 3T88

(b) Amino Acid Interaction of Molecule D23 on 3T88



(b)

According to molecular docking studies and interaction between protein and designed molecule D17 have Moldock score **-130.676** with amino acid interactions Arg64, Arg230, Glu248, Gln114, Thr117, and Asp110 molecule D23 have Moldock score **-126.828** with amino acid interactions Thr117, Arg230, Asn252, Arg64, Asp110, Arg64, and Met25.

**Drug likeness and in-silico ADMET:** Table 4 showcases that the majority of the 1,3,4-thiadiazole Ciprofloxacin derivatives exhibit favorable drug-like characteristics across various parameters. These parameters typically conform to the established drug-likeness criteria, including a molecular weight (MW) under 500 Da, a LogP below 5, fewer than 5 hydrogen bond donors (nHBD), fewer than 10 hydrogen bond acceptors (nHBA), and a total polar surface area (TPSA) below 140 Å<sup>2</sup>.

However, compounds that violate two or more of Lipinski's Rule of Five parameters might indicate oral inaccessibility. Additionally, the Log S values for all derivatives fall between 7.12 and 9.10, indicating poor solubility in water for these compounds. Conversely, a TPSA value below 140 for most compounds suggests excellent absorption in the intestine.

Stereo-specificity, reflected in nRotB values, remains less than 10 for the majority of the molecules. Lipinski's Rule of Five serves as an assessment tool to gauge the oral activity of active compounds. Parameters such as



Log P, TPSA, MW, HBA, and HBD indicate oral bioavailability by influencing membrane permeability and the hydrophobicity of the drug molecules. Furthermore, favorable values of nRotB and molecular

refractivity (MR) correspond to good intestinal absorption and oral bioavailability for some of these compounds.

**Table 4:** Represent the ADME properties that have been determined using Swiss ADME:

S. No.	Molecule	M.W.	LogP o/w	Lipinski's violations	Rotatable bonds	H-bond acceptors	H-bond donors	Molar Refractivity	TPSA	Log S
1.	D1	640.84	3.07	1	8	6	1	167.1	136.9	-6.24
2.	D2	605.53	4.51	1	11	7	2	184.02	136.9	-6.87
3.	D3	554.63	3.58	1	12	12	1	188.35	136.9	-5.45
4.	D4	568.66	4.1	1	16	7	1	197.22	136.9	-6.1
5.	D5	615.54	3.91	1	10	10	1	163.16	136.9	-6.08
6.	D6	564.7	4.11	1	9	8	1	155.96	136.9	-5.67
7.	D7	596.7	3.77	1	9	7	2	158.67	155.36	-5.5
8.	D8	626.64	2.44	1	9	9	2	157.18	237.33	-5.15
9.	D9	581.64	2.99	1	8	6	1	172.48	191.51	-5.07
10.	D10	581.64	2.99	1	10	11	3	165.45	191.51	-5.07
11.	D11	595.67	3.12	1	9	7	1	160.38	182.72	-5.44
12.	D12	568.71	3.72	1	9	6	1	176.35	184.49	-5.28
13.	D13	664.86	5.85	1	15	7	1	192.41	136.9	-5.61
14.	D14	606.78	5.02	1	8	6	2	159.43	136.9	-6.66
15.	D15	581.64	3.04	1	9	8	1	165.9	182.72	-5.72
16.	D16	628.66	2.48	1	9	8	2	161	228.54	-6.36
17.	D17	708.46	5.03	1	9	8	2	161	136.9	-7.77
18.	D18	604.64	4.6	1	10	10	2	169.82	145.69	-5.87
19.	D19	566.67	3.29	1	10	8	1	164.65	145.69	-4.99
20.	D20	567.66	2.81	1	8	6	1	162.04	158.58	-4.33
21.	D21	634.67	4.55	1	8	6	1	160.14	145.69	-5.87
22.	D22	678.88	6.15	1	8	7	1	157.04	145.69	-4.99
23.	D23	699.69	2.14	1	8	7	1	152.32	274.36	-5.85
24.	D24	635.82	4.12	1	8	6	1	162.08	162.92	-5.83
25.	D25	619.56	4.88	1	9	12	5	178.44	136.9	-7.13

### Conclusion:

The escalating threat posed by bacterial infections, compounded by their growing resistance to antimicrobial treatments, presents a substantial global health concern. To address this challenge, our study focused on designing derivatives of Ciprofloxacin-based 1,3,4 thiadiazole compounds, aiming to enhance their antimicrobial efficacy. Through assessments on target proteins 4KRA and 3T88, certain proposed compounds displayed superior binding interactions, as evaluated

using the Molegro Virtual Docker software. Our investigations, incorporating docking simulations, drug-likeness evaluations, and ADMET analyses of these Ciprofloxacin derivatives in the 1,3,4 thiadiazole series, underscored the significance of hydrogen bonding and other molecular interactions within all the compounds. Notably, molecules D14 and D23 exhibited exceptional stability, displaying dock scores of 154.547 and 142.085 against the 4KRA protein. Additionally, molecules D17 and D23 showcased notable stability, with dock scores of



130.676 and 126.129 against the 3T88 protein, rivaling the performance of standard drugs.

These compounds not only demonstrated favorable Lipinski parameters but also showcased poor aqueous solubility coupled with impressive permeability across biological membranes and the gastrointestinal tract (GIT). The findings from this study lay a foundational framework for further optimization of Ciprofloxacin 1,3,4 thiadiazole derivatives, aiming to enhance their interactions with receptors and develop more potent antibacterial agents.

#### Experimental section:

- Generation of Free Ciprofloxacin from Ciprofloxacin HCl-** Ciprofloxacin hydrochloride (4.0 g, 13.59 mmol) was dissolved in water (30 mL) to get a clear solution. This solution was treated with an excess of 5% aqueous sodium bicarbonate solution, resulting in the formation of a white precipitate. The precipitate was filtered off and dry as a free 1-cyclopropyl-6-fluoro-4-oxo-7-piperazin-1-ylquinoline-3- carboxylic acid (ciprofloxacin 1, 3.3 g, 12.98 mmol). The free ciprofloxacin was pure enough and used as starting material for the further reaction without purification. White solid, yield 3.9 g.
- General Procedure for the Synthesis of 1,3,4-thiadiazole Scaffolds-** The synthesis of thiadiazole was carried out according to the published procedure. Briefly, 1- cyclopropyl-6-fluoro-4-oxo-7-(4-prop-2-ynyl-piperazin-1-yl)- 1,4-dihydroquinoline-3- carboxylic acid methyl/ethyl/propyl ester and thiosemicarbazide derivative (2.0 g, 0.074 mol), and  $\text{POCl}_3$  (20 ml 0.222 mol) were stirred under reflux for 4 hours at 90 °C. The cooled product precipitated with ice water. The neutralized mixture with ammonia solution was left in the refrigerator overnight. Final material was filtered and washed, then dried using a vacuum oven and crystallized in DMF/water (2:1) mixture. Finally, the obtained product was treated with substituted benzyl mercaptan (5.0 ml, 1.303 mol) to get the substituted 1,3,4-thiadiazole derivatives of ciprofloxacin. Other compounds were performed using the same procedure.

#### References:

- Tehranchian S., Akbarzadeh T., Fazeli M.R., Jamalifar H., Shafiee A. Synthesis and antibacterial activity of 1-[1,2,4-triazol-3-yl] and 1-[1,3,4-thiadiazol-2-yl]-3-methylthio-6,7-dihydrobenzo[c]thiophen-4(5H) ones. *Bioorg. Med. Chem. Lett.* 2005; 15:1023–1025. doi: 10.1016/j.bmcl.2004.12.039. [PubMed] [CrossRef] [Google Scholar]
- Caleb A.A., Ballo D., Rachid B., Amina H., Mostapha B., Abdelfettah Z., Mokhtar E.E. Synthesis and antibacterial activity of new spiro[thiadiazoline-quinoline] derivatives. *Arkivoc.* 2011; 2:217–226. [Google Scholar]
- Narendhar B., Alagarsamy V., Krishnan C. Design and Synthesis of novel 1-substituted-3-(3-(3-nitrophenyl)-4-oxo-3,4-dihydrobenzopyrimidin-2-ylamino) isothioureas for their anti-HIV, antibacterial activities, graph theoretical analysis, in silico modeling, prediction of toxicity and metabolic studies. *Drug Res.* 2020; 70:348–355. [PubMed] [Google Scholar]
- Toan V.N., Tri N.M., Thanh N.D. Substituted 4-formyl-2H-chromen-2-ones: Their reaction with N-(2,3,4,6-tetra-O-acetyl-β-D-galactopyranosyl) thiosemicarbazide, antibacterial and antifungal activity of their thiosemicarbazone products. *Curr. Org. Chem.* 2020; 24:2272–2282. doi: 10.2174/1385272824999200812132256. [CrossRef] [Google Scholar]
- Molnar M., Tomić M., Pavić V. Coumarinyl thiosemicarbazides as antimicrobial agents. *Pharm. Chem. J.* 2018; 51:1078–1081. doi: 10.1007/s11094-018-1743-3. [CrossRef] [Google Scholar]
- Muğlu H., Akın M., Çavuş M.S., Yakan H., Şaki N., Güzel E. Exploring of antioxidant and antibacterial properties of novel 1,3,4-thiadiazole derivatives: Facile synthesis, structural elucidation and DFT approach to antioxidant characteristics. *Comput. Biol. Chem.* 2022; 96:107618. doi: 10.1016/j.compbiolchem.2021.107618. [PubMed] [CrossRef] [Google Scholar]
- Ernazarova B., Zhusubaliev T., Bakirova A., Zhusupbaeva G., Akparalieva O., Abdullaeva Z., Orozmatova A. Study of Biological Activity and Toxicity of Thiosemicarbazides Carbohydrate Derivatives by in Silico, In Vitro and In Vivo Methods. *J. Agric. Chem. Environ.* 2022;11:15–23. [Google Scholar]

1. Tehranchian S., Akbarzadeh T., Fazeli M.R.,



8. Bhakiaraj D., Elavarasan T., Mathavan M., Megala S., Enbaraj E., Gopalakrishnan M. Synthesis, spectral analysis, antibacterial activity and molecular docking studies of some novel derivatives of combined tetrazole and thiosemicarbazide moieties. *J. Adv. Sci. Res.* 2021;12:210–218. doi: 10.55218/JASR.s1202112423. [CrossRef] [Google Scholar]
9. Han M.İ., İnce U., Gündüz M.G., Küçükgül Ş.G. Synthesis, Antimicrobial Evaluation, and Molecular Modeling Studies of New Thiosemicarbazide-Triazole Hybrid Derivatives of (S)-Naproxen. *Chem. Biodivers.* 2022;19:e202100900. doi: 10.1002/cbdv.202100900. [PubMed] [CrossRef] [Google Scholar]
10. Sriram D., Yogeewari P., Thirumurugan R., Pavana R.K. Discovery of new antitubercular oxazolyl thiosemicarbazones. *J. Med. Chem.* 2006;49:3448–3450. doi: 10.1021/jm060339h. [PubMed] [CrossRef] [Google Scholar]
11. García C.C., Brousse B.N., Carlucci M.J., Moglioni A.G., Alho M.M., Moltrasio G.Y., Damonte E.B. Inhibitory effect of thiosemicarbazone derivatives on Junin virus replication in vitro. *Antivir. Chem. Chemother.* 2003;14:99–105. doi: 10.1177/095632020301400205. [PubMed] [CrossRef] [Google Scholar]
12. Plech T., Wujec M., Siwek A., Kosikowska U., Malm A. Synthesis and antimicrobial activity of thiosemicarbazides, s-triazoles and their Mannich bases bearing 3-chlorophenyl moiety. *Eur. J. Med. Chem.* 2011;46:241–248. doi: 10.1016/j.ejmech.2010.11.010. [PubMed] [CrossRef] [Google Scholar]
13. Kalhor M., Shabani M., Nikokar I., Banisaeed S.R. Synthesis, characterization and antibacterial activity of some novel thiosemicarbazides, 1,2,4-triazol-3-thiols and their S-substituted derivatives. *Iran J. Pharm. Res.* 2015;14:67. [PMC free article] [PubMed] [Google Scholar]
14. Bhat M.A., Khan A.A., Ghabbour H.A., Quah C.K., Fun H.K. Synthesis, characterization, x-ray structure and antimicrobial activity of N-(4-chlorophenyl)-2-(pyridin-4-ylcarbonyl) hydrazinecarbothioamide. *Trop. J. Pharm. Res.* 2016;15:1751–1757. doi: 10.4314/tjpr.v15i8.22. [CrossRef] [Google Scholar]
15. Li Y., Geng J., Liu Y., Yu S., Zhao G. Thiadiazole—A promising structure in medicinal chemistry. *ChemMedChem.* 2013;8:27–41. doi: 10.1002/cmdc.201200355. [PubMed] [CrossRef] [Google Scholar]
16. Siwek A., Stączek P., Wujec M., Stefańska J., Kosikowska U., Malm A., Paneth P. Biological and docking studies of topoisomerase IV inhibition by thiosemicarbazides. *J. Mol. Model.* 2011;17:2297–2303. doi: 10.1007/s00894-010-0889-z. [PubMed] [CrossRef] [Google Scholar]
17. Kowalczyk A., Paneth A., Trojanowski D., Paneth P., Zakrzewska-Czerwińska J., Stączek P. Thiosemicarbazide Derivatives Decrease the ATPase Activity of Staphylococcus aureus Topoisomerase IV, Inhibit Mycobacterial Growth, and Affect Replication in Mycobacterium smegmatis. *Int. J. Mol. Sci.* 2021;22:3881. doi: 10.3390/ijms22083881. [PMC free article] [PubMed] [CrossRef] [Google Scholar]
18. Plech T., Paneth A., Kaproń B., Kosikowska U., Malm A., Strzelczyk A., Stączek P. Structure–activity Relationship studies of microbiologically active thiosemicarbazides derived from hydroxybenzoic acid hydrazides. *Chem. Biol. Drug. Des.* 2015;85:315–325. doi: 10.1111/cbdd.12392. [PubMed] [CrossRef] [Google Scholar]
19. Paneth A., Stączek P., Plech T., Strzelczyk A., Dzitko K., Wujec M., Paneth P. Biological evaluation and molecular modelling study of thiosemicarbazide derivatives as bacterial type IIA topoisomerases inhibitors. *J. Enzyme Inhib. Med. Chem.* 2016;31:14–22. doi: 10.3109/14756366.2014.1003214. [PubMed] [CrossRef] [Google Scholar]
20. Janowska S., Khylyuk D., Bielawska A., Szymanowska A., Gornowicz A., Bielawski K., Noworól J., Mandziuk S., Wujec M. New 1,3,4-Thiadiazole Derivatives with Anticancer Activity. *Molecules.* 2022;27:1814. doi: 10.3390/molecules27061814. [PMC free article] [PubMed] [CrossRef] [Google Scholar]
21. Murray C.J., Ikuta K.S., Sharara F., Swetschinski L., Aguilar G.R., Gray A., Naghavi M. Global burden of bacterial antimicrobial resistance in 2019: A systematic analysis. *Lancet.* 2022;399:629–655. doi: 10.1016/S0140-6736(21)02724-0. [PMC free article] [PubMed] [CrossRef] [Google Scholar]



22. Germe T., Vörös J., Jeannot F., Taillier T., Stavenger R.A., Bacqué E., Bax B.D. A new class of antibacterials, the imidazopyrazinones, reveal structural transitions involved in DNA gyrase poisoning and mechanisms of resistance. *Nucleic Acids Res.* 2018;46:4114–4128. doi: 10.1093/nar/gky181. [PMC free article] [PubMed] [CrossRef] [Google Scholar]
23. Laponogov I., Pan X.S., Veselkov D.A., McAuley K.E., Fisher L.M., Sanderson M.R. Structural basis of gate-DNA breakage and resealing by type II topoisomerases. *PLoS ONE.* 2010;5:11338. doi: 10.1371/annotation/deacc2fd-665b-4736-b668-dc69a38bb4f9. [PMC free article] [PubMed] [CrossRef] [Google Scholar]
24. CLSI . Performance Standards for Antimicrobial Susceptibility Testing. 32nd ed. Volume 42. Clinical Lab Standards Institute; Malvern, PA, USA: 2022. pp. 34–78. CLSI Supplement M100. [Google Scholar]
25. Hashem H.E., Amr A.E.G.E., Nossier E.S., Elsayed E.A., Azmy E.M. Synthesis, antimicrobial activity and molecular docking of novel thiourea derivatives tagged with thiadiazole, imidazole and triazine moieties as potential DNA gyrase and topoisomerase iv inhibitors. *Molecules.* 2020;25:2766. doi: 10.3390/molecules25122766. [PMC free article] [PubMed] [CrossRef] [Google Scholar]
26. El-Hachem N., Haibe-Kains B., Khalil A., Kobeissy F.H., Nemer G. *Neuroproteomics.* Humana Press; New York, NY, USA: 2017. AutoDock and AutoDockTools for protein-ligand docking: Beta-site amyloid precursor protein cleaving enzyme 1 (BACE1) as a case study; pp. 391–403. [PubMed] [Google Scholar]